



An Improved Particle Finite Element Method for the Simulation of Machining Processes

Xialong Ye¹  

Applied Mechanics, Technische Universität Kaiserslautern, Germany

Juan Manuel Rodríguez Prieto

Mechanical Engineering Department, Universidad EAFIT, Medellín, Colombia

Ralf Müller

Applied Mechanics, Technische Universität Kaiserslautern, Germany

Abstract

Machining is one of the most common and versatile manufacturing processes in industry, e.g. automotive industry and aerospace industry. But classical numerical methods such as the Finite Element Method (FEM) have difficulties to simulate it, because the material undergoes large deformations, large strain, large strain rates and high temperatures in this process. One option to simulate such kind of problems is the Particle Finite Element Method (PFEM) which combines the advantages of continuum mechanics and discrete modeling techniques. In this study we develop the PFEM further and call it the Adaptive Particle Finite Element Method (A-PFEM). Compared to the PFEM the A-PFEM enables insertion of particles and improves significantly the mesh quality along the numerical simulation. The A-PFEM improves accuracy and precision, while it decreases computing time and resolves the phenomena that take place in machining. Because metal cutting involves plastic deformation we resort to the J_2 flow theory with isotropic hardening. At last some numerical examples are presented to compare the performance of the PFEM and A-PFEM.

2012 ACM Subject Classification Applied computing → Physical sciences and engineering

Keywords and phrases Particle Finite Element Method, Alpha Shape Method, Metal Cutting

Digital Object Identifier 10.4230/OASICS.iPMVM.2020.13

Funding This research is funded by the Deutsche Forschungsgemeinschaft (DFG German Research Foundation) - 252408385 - IRTG 2057.

1 Instruction

Machining is a subtractive manufacturing process. Material is removed from a workpiece by a machining tool to obtain a desired shape. It is the most common and versatile manufacture processes in automotive and aerospace industry. The experimental approach to study this process is very expensive and time consuming. Therefore, numerical simulations seem to be another option. The most widely used numerical method for solving problems of engineering is the Finite Element Method (FEM) [4], which is appropriate for modelling of complex material behaviour but problematic for large configurational changes. That is because the result of the FEM is highly dependent on the quality of the mesh [15]. In machining process the material undergoes large deformations and large configurational changes. If we use a Lagrangian formulation, the mesh moves with the material and the elements become so distorted that some elements may have negative Jacobian and the numerical simulation breaks down [7]. A possible alternative is using meshless methods such as molecular dynamics (MD) and material point method (MPM), which are suitable for simulation of problems with large configurational changes, but the main disadvantage is that they are computationally

¹ corresponding author

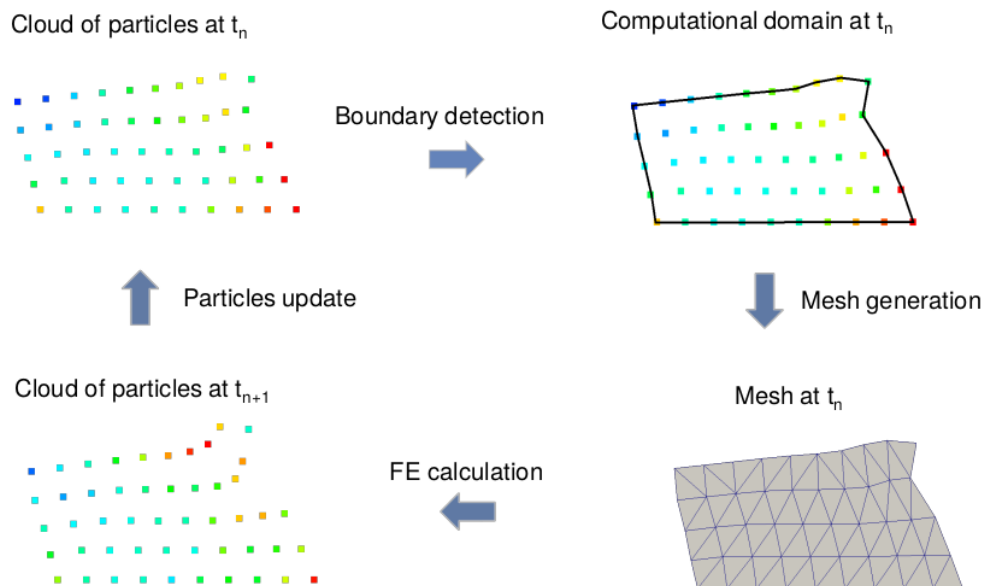


expensive for large length and time scales. The Particle Finite Element Method (PFEM) which was first applied for problems with liquid solid interaction combines the benefits of the FEM and the meshless methods [5]. During the simulation by using the PFEM the boundary is repeatedly detected by the α -shape method, which is appropriate for the simulation of cutting process. The domain is continuously remeshed, which make simulations with large configurational changes possible [11]. But PFEM still has some difficulties in machining simulations. In most PFEM simulations the number of the particles is fixed along the simulation, that gives rise to dense distribution of particles in some regions meanwhile sparse distribution of particles in other regions. The reported situation generates low quality of the finite elements and in some cases spurious holes. To improve the PFEM an Adaptive Particle Finite Element Method (A-PFEM) is introduced, which enables insertion of particles where the elements become too large during the simulation. Moreover a node to surface strategy is applied to solve the contact problem in this work, so near the tool tip some elements may overlap with the tool. This kind of elements should be removed.

The outline of this work is as follows. In section 2 an overview of the PFEM is illustrated. An improved PFEM called A-PFEM is introduced. In section 3 the constitutive model used in this work is explained. In the last section a couple of numerical simulations are demonstrated to show the efficiency of the proposed method.

2 Particle finite element method (PFEM)

The PFEM initially implemented for fluid mechanics problems is also a powerful tool for simulation of solid mechanics [12]. For PFEM an updated Lagrangian approach is applied to track the motion of the particles and a remeshing technique is used to overcome the problem of mesh distortion [8]. An overview of the PFEM is illustrated in Fig. 1. The computational

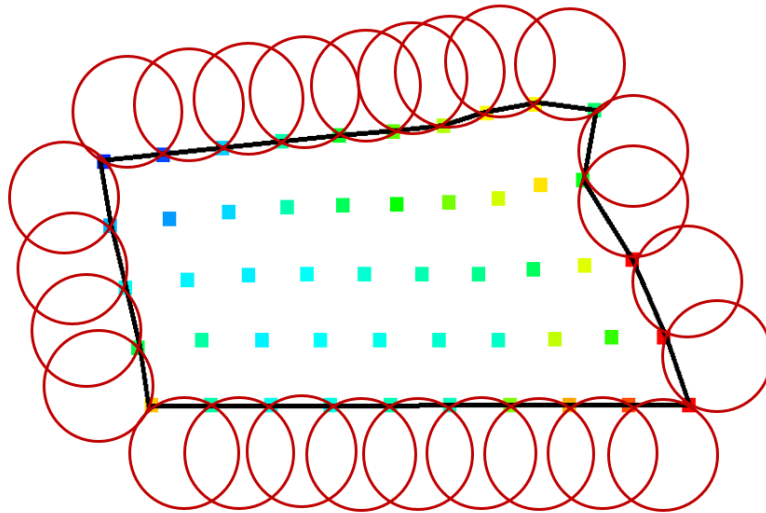


■ **Figure 1** Operations in a standard PFEM algorithm.

domain is represented by a cloud of particles, which carry the physical quantities such as the deformation gradient, plastic deformation gradient and hardening variables. Different color of particles means different value of the physical quantities. The boundary of the particles is identified by using the so called α -shape method [2], that we will elaborate in the following subsection. For the FEM calculation we still need a finite element mesh. In this work we use the program triangle [13] to mesh the domain and the finite element programme FEAP [14] to solve the finite element problem. After that we update the particle position by using the result of the displacement obtain from the FEM calculation and project the physical quantities from the Gauß points to the particles for the next time step.

2.1 Alpha shape method

One of the key technique in the PFEM is the α -shape method, which stems from the field of computational geometry [3]. There are two versions of the α -shape method. We name them α -shape method 1 and 2 respectively for the following. For α -shape method 1 let S be the set of the particles defining the domain and h_{min} is the smallest distance between any two particles in S . For every pair of particles in S there may be two circles with radius αh_{min} that intersect both particles. If there is at least one of the both circles empty, i.e. no other particles are located within the circle, the two particles form a boundary segment. Here α is the crucial parameter which controls the shape of the detected boundary. For a uniform distribution of particles the value of α between 1.1 and 1.5 provides a good estimation of the boundary [12]. An example of this kind of α -shape method is illustrated in Fig. 2. The



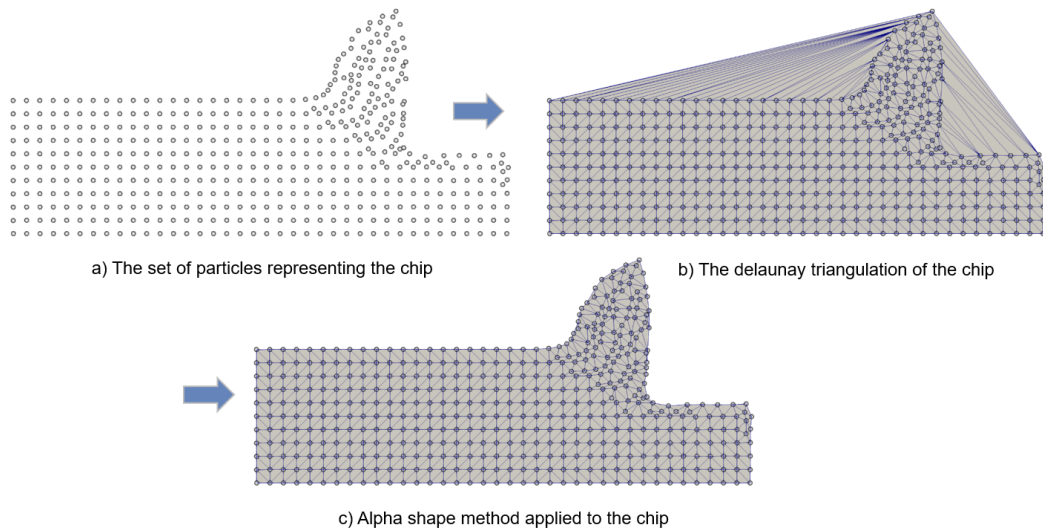
■ **Figure 2** α -circles and the detected boundary.

problem of the α -shape method 1 is that the particles cannot keep uniform distribution along the machining process. Some particles move to each other, so that h_{min} tends to be zero. Therefore if the above α -shape method is adopted in the PFEM, the particles should be uniform distributed at the initial state and the h_{min} is only calculated once at the first time step and keep it invariant during the following simulation [13]. This version of the α -shape method may work in the PFEM, but the smallest distance h_{min} lost its meaning after the first time step.

Whereas in the α -shape method 2 the detected shape depends locally only the particles surrounding it [10]. That means for this version the particles don't need to be uniform distributed. For that we use the Delaunay triangulation to mesh the particles first and remove the unnecessary triangles for obtaining the shape of the particles. This can be achieved as following. For every element e let h_e be the smallest distance of two particles in element e and r_e be the radius of the circumcircle of the element e . For every node n let h_n be the mean value of h_e for all element surrounding this node. The distortion index α_e of the element e can be defined as

$$\alpha_e = \frac{r_e}{h_{ave}}, \quad (1)$$

where h_{ave} is the mean value of h_n for element e . For all elements if $\alpha_e > \alpha$ it will be removed, here α is the crucial parameter. An example of the α -shape method 2 is shown in Fig. 3.

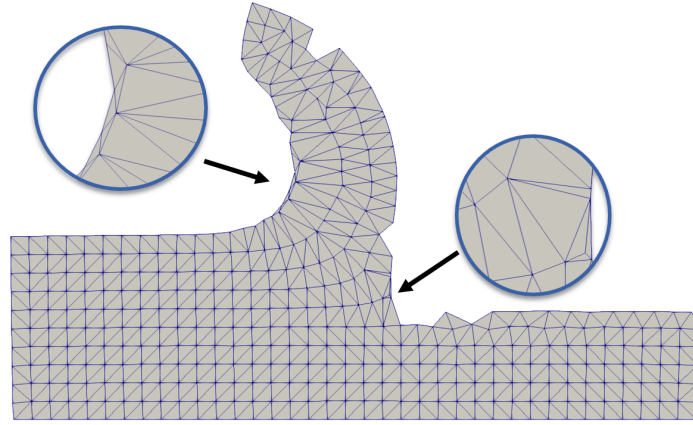


■ **Figure 3** The steps in α -shape method 2.

2.2 Adaptive particle finite element method (A-PFEM)

The PFEM is a powerful tool thanks to the repetitive boundary detection and remeshing procedure, but still has difficulties in the numerical simulation of metal cutting process. It is impossible to avoid the presence of poor quality elements, that means the elements have small aspect ratios, and in some cases artificial holes appear as shown in Fig. 4. That is because keeping the same number of particles along the numerical simulation results in a nonuniform distribution of particles. In some regions the distribution becomes very dense meanwhile in other regions it becomes very sparse.

To overcome this difficulty the Gauß point can be inserted as a new particle in elements which become too large, that means if the area of a element is larger than μ times the initial area of this element a Gauß point will be inserted. In this work we set $\mu = 1.03$. The information of the new inserted particles can be approximated by interpolation of the



■ **Figure 4** Artificial hole and low quality elements from a standard PFEM simulation.

surrounding particles. For simplicity the internal variables for the new particles are the internal variables available at the old Gauß points from solving the FEM problem in the last time step.

To solve the contact problem we use a node to surface strategy. So we shall especially pay attention to the nodes near the tool tip. It may occur that an element overlaps with the tool. For that we check every element. If 2 nodes of a element locate on the boundary of the tool and its centroid locates inside the tool, this element will be removed. In summary, comparing to the PFEM the A-PFEM removes bad elements after the mesh generation and inserts adaptively new points after the FE calculation in every time step.

3 The constitutive model

Nonlinear plasticity plays a key role in metal cutting. In this work we introduce a phenomenological plasticity model namely J_2 flow theory with isotropic hardening [6]. Furthermore, it is assumed that plastic flow is isochoric in accordance with the standard assumption in metal plasticity. For plasticity a multiplicative decomposition of the deformation gradient

$$\mathbf{F} = \mathbf{F}^e \mathbf{F}^p \quad (2)$$

was first introduced in [9], where \mathbf{F}^e and \mathbf{F}^p are the elastic and the plastic part, respectively. A stored-energy function is given by

$$W(J^e, \bar{\mathbf{b}}^e) = U(J^e) + \bar{W}(\bar{\mathbf{b}}^e) \quad (3)$$

with the volumetric part $U(J^e)$ and the deviatoric part $\bar{W}(\bar{\mathbf{b}}^e)$ defined by

$$U(J^e) = \frac{\kappa}{2} \left[\frac{1}{2} (J^{e2} - 1) - \ln J^e \right] \quad \text{and} \quad \bar{W}(\bar{\mathbf{b}}^e) = \frac{1}{2} \mu (\text{tr}[\bar{\mathbf{b}}^e] - 3), \quad (4)$$

where $J^e = \det[\mathbf{F}^e]$, $\bar{\mathbf{b}}^e = J^{e-\frac{2}{3}} \mathbf{F}^e \mathbf{F}^{eT}$. Here κ and μ are shear modulus and the bulk modulus, respectively. From Eq. (3) the Kirchhoff stress tensor $\boldsymbol{\tau}$ is derived as

$$\boldsymbol{\tau} = J^e p \mathbf{1} + \mathbf{s}, \quad (5)$$

13:6 An Improved PFEM for the Simulation of Machining Processes

with the Kirchhoff pressure p and the deviatoric component of the Kirchhoff stress tensor \mathbf{s} defined as

$$p = U'(J^e) = \frac{\kappa}{2}(J^e - \frac{1}{J^e}) \quad \text{and} \quad \mathbf{s} = \text{dev}[\boldsymbol{\tau}] = \mu \text{dev}[\bar{\mathbf{b}}^e]. \quad (6)$$

The yield condition, the associate flow rule and the isotropic hardening law, respectively, take the form

$$f(\boldsymbol{\tau}, \alpha) = \|\text{dev}[\boldsymbol{\tau}]\| - \sqrt{\frac{2}{3}}[\sigma_Y + K\alpha], \quad (7)$$

$$\frac{d}{dt} \{\bar{\mathbf{C}}^{p-1}\} = -\frac{2}{3}\gamma \text{tr}[\mathbf{b}^e] \mathbf{F}^{-1} \mathbf{n} \mathbf{F}^{-T}, \quad (8)$$

$$\dot{\alpha} = \sqrt{\frac{2}{3}}\gamma, \quad (9)$$

where $\mathbf{n} := \frac{\mathbf{s}}{\|\mathbf{s}\|}$, σ_Y denotes the initial yield stress, K the isotropic hardening modulus, α the hardening variable, $\bar{\mathbf{C}}$ the volume-preserving part of the right Cauchy-Green tensor \mathbf{C} , and γ the flow rate, which can be derived from the Kuhn-Tucker conditions and consistency condition:

$$\gamma \geq 0, \quad f(\boldsymbol{\tau}, \alpha) \leq 0, \quad \gamma f(\boldsymbol{\tau}, \alpha) = 0, \quad (10)$$

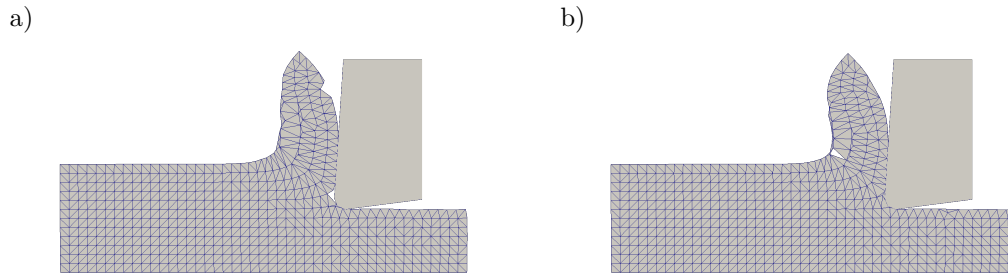
$$\gamma \dot{f}(\boldsymbol{\tau}, \alpha) = 0 \quad \text{if} \quad f(\boldsymbol{\tau}, \alpha) = 0. \quad (11)$$

4 Numerical examples

In this section we show the performance of numerical methods introduced in the previous sections. All the following simulations are based on a cutting process for a material with Young's modulus $E = 210$ GPa, Poissons ratio $\nu = 0.3$, initial yield stress $\sigma_Y = 450$ MPa and hardening modulus $K = 129$ MPa. The above parameters are used to mimic steel. In this cutting process the tool is fixed and the workpiece moves towards the tool [1]. For simplicity we let the cutting tool be a rigid body and there is only normal contact between tool and workpiece. A contour plot of the normal stresses σ_{xx} will be illustrated. In the FEM we use a linear 3-node triangle element.

4.1 PFEM with two different α -shape method

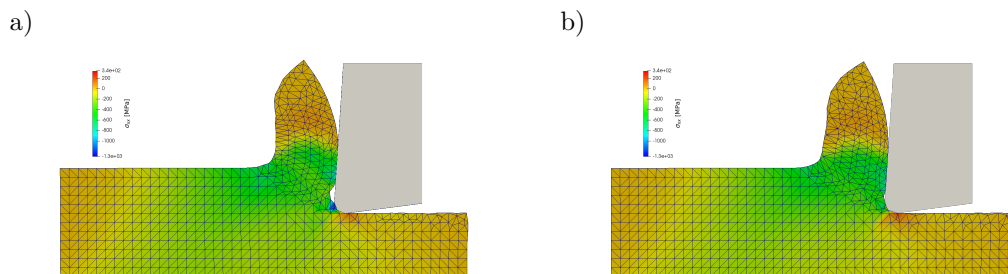
First we use the PFEM with α -shape method 1 and 2 respectively and only focus on the quality of the mesh. In Fig. 5 it can be observed that a "sawtooth" formed by using the α -shape method 1 and a hole formed by using α -shape method 2. The first phenomenon occurs because the radius of the α -circles is only defined for the initial state and too small for some later iterations. The second phenomenon happens because the local information around the hole is not correct. Besides it can be obviously seen in both examples that there are a lot of poor quality elements that have very small aspect ratio, inside the chip. Both methods can be made valid by inserting new particles in the appreciate positions along the simulation.



■ **Figure 5** PFEM simulation using a) α -shape method 1 and b) α -shape method 2.

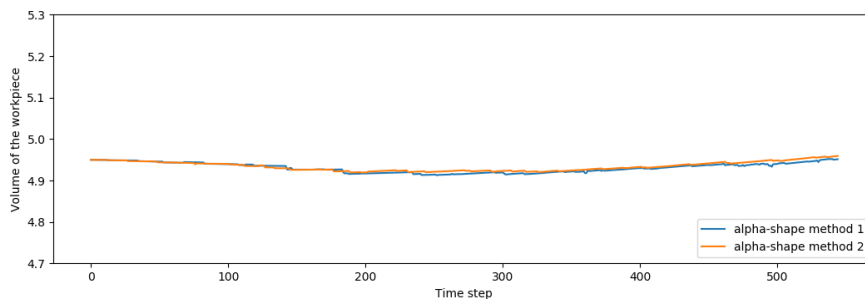
4.2 A-PFEM with two different α -shape method

We use the A-PFEM with α -shape method 1 and 2 respectively. A normal stress σ_{xx} is plotted. As illustrated in Fig. 6 high compressive stresses occur in front of the cutting tool. Comparing to the previous numerical examples both the “sawtooth” and the the hole



■ **Figure 6** σ_{xx} stress using A-PFEM with a) α -shape method 1 and b) α -shape method 2.

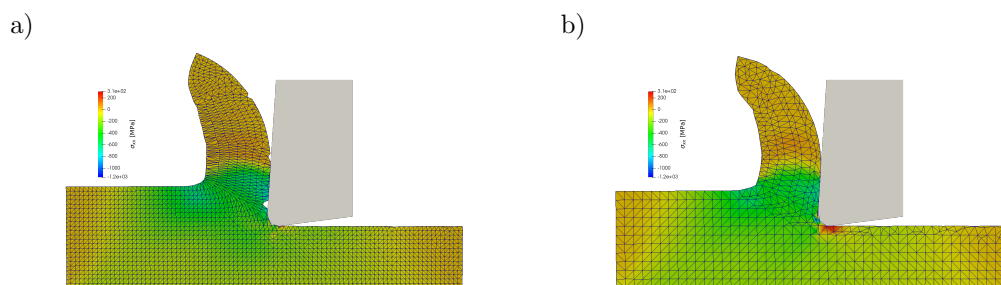
don't appear. The elements with small aspect ratio also never show up due to the adaptive insertion of the particles. We also plot the volume of the workpiece with respect to the time step. The initial volume is 4.95. Since the workpiece has constant density, Fig. 7 shows the mass conservation for both methods.



■ **Figure 7** Workpiece volume during the A-PFEM simulation with α -shape method 1 and 2.

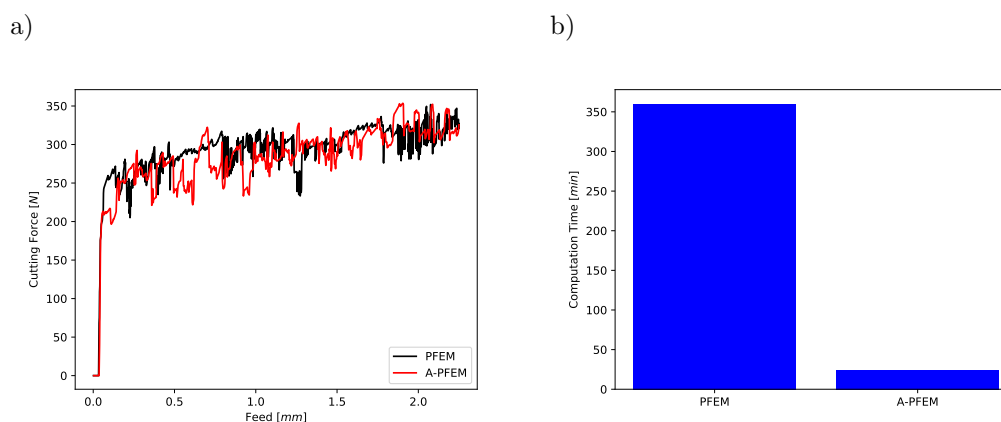
4.3 Comparison of PFEM and A-PFEM

We want to compare the performance of the PFEM and the A-PFEM from various aspects. For this purpose we start the cutting simulation by using the A-PFEM with much fewer particles as the simulation by using the PFEM. The normal stresses are plotted. Fig. 8 shows



■ **Figure 8** σ_{xx} stress using a) PFEM with refined discretisation and b) A-PFEM with coarse discretisation.

that the derived contour of both method are almost the same apart from the “sawteeth” in Fig. 8a). In Fig. 8b) it can also be observed that the inserted particles are mainly placed where the cutting process occurs and the aspect ratios of the elements in A-PFEM are obviously much smaller. Fig. 9a) shows a plot of the cutting forces of PFEM and A-PFEM. Fig. 9b) shows the computation time of PFEM and A-PFEM. Their cutting forces meet each other but the computation time by using the A-PFEM is much shorter. That is because fewer particles lead to fewer elements, and fewer elements mean a faster solution of the FEM problem, which requires most of the computation time in the simulation. In the example with A-PFEM 717 particles and 1274 elements are used comparing that 2191 particles and 4146 elements in the example with PFEM.



■ **Figure 9** Comparison of a) the cutting force and b) the computation time.

5 Conclusion

An improved particle finite element method (PFEM) called adaptive particle finite element method (A-PFEM) is established in this work. In contrast to the PFEM the A-PFEM inserts new particles adaptively along the numerical simulation. In the A-PFEM the distribution of particles, which represent the computation domain, is smoother. This leads to a reduction of computing time, because we can start with fewer particles by using the A-PFEM. The new particles will be inserted in the appropriate place during the simulation, and we get the same

quality of the results as we use the PFEM with more particles. The newly developed A-PFEM is much more efficient than the PFEM and generates better meshes. Moreover, two kinds of α -shape method are discussed in this work. The α -shape method 2 is more reasonable for the simulation of the machining process, because the distribution of the particles cannot keep uniform during the simulation. In α -shape method 2 the detected shape of the particles only depends on the particles near it. For the nonlinear plasticity problem a J_2 flow theory with isotropic hardening model was introduced.

References

- 1 H. K. Toenshoff B. Denkena. *Spanen*. Springer-Verlag, 2011.
- 2 K. Fischer. Introduction to alpha shapes. *Department of Information and Computing Sciences, Faculty of Science, Utrecht University*, 2000.
- 3 E. P. Mücke H. Edelsbrunner. Three-dimensional alpha shapes. *ACM Transactions on Graphics*, 13(1):43–72, 1994.
- 4 G. Holzapfel. *Nonlinear Solid Mechanics*. John Wiley & Sons, 2001.
- 5 S. R. Idelsohn, E. Oñate, F. Del Pin, and N. Calvo. The particle finite element method. an overview. *International Journal of Computational Methods*, 1(2):267–307, 2004.
- 6 T.J.R. Hughes J. C. Simo. *Computational Inelasticity*, volume 7. Springer Science & Business Media, 2006.
- 7 A. Svoboda J. M. Rodriguez, P. Jonsén. A particle finite element method for machining simulations. *VII European Congress on Computational Methods in Applied Sciences and Engineering, Crete Island, Greece, 5–10 June 05/06/2016-10/06/2016*, 1:539–553, 2016.
- 8 A. Svoboda J.M. Rodriguez, P. Jonsén. Simulation of metal cutting using the particle finite-element method and a physically based plasticity model. *Computational Particle Mechanics*, 4:35–51, 2017.
- 9 E. H. Lee. Elastic-plastic deformation at finite strains. *Journal of Applied Mechanics*, 36(1):1–6, 1969.
- 10 A. Frangi M. Cremonesi and U. Perego. A lagrangian finite element approach for the analysis of fluid–structure interaction problems. *INTERNATIONAL JOURNAL FOR NUMERICAL METHODS IN ENGINEERING*, 84:610–630, 2010.
- 11 R. Müller M. Sabel and C. Sator. Simulation of cutting processes by the particle finite element method. *GAMM-Mitteilungen*, 40(1):51–70, 2017.
- 12 J. Oliver, J.C. Cante, R. Weyler, C. González, and J. Hernández. Particle finite element methods in solid mechanics problems. *Computational plasticity*, pages 87–103, 2007.
- 13 J. R. Shewchuk. Triangle: Engineering a 2d quality mesh generator and delaunay triangulator. *Applied Computational Geometry: Towards Geometric Engineering*, pages 203–222, 1996.
- 14 R. L. Taylor. Feap - a finite element analysis program: User manual. *Department of Civil and Environmental Engineering, University of California, Berkley*, 2009.
- 15 P. Wriggers. *Nonlinear finite element methods*. Springer Science & Business Media, 2008.